frontiers | Frontiers in Marine Science

TYPE Original Research
PUBLISHED 13 June 2025
DOI 10.3389/fmars.2025.1621833

OPEN ACCESS

EDITED BY
Meilin Wu,
Chinese Academy of Sciences (CAS), China

REVIEWED BY
Junliang Gao,
Jiangsu University of Science and Technology, China
Jianhuang Qin,
Hohai University, China
Zhixiong Yao,
Ministry of Natural Resources, China

*CORRESPONDENCE
Peng Bai
pengbai@zjou.edu.cn
Mingming Li
limm@gdou.edu.cn

RECEIVED 02 May 2025
ACCEPTED 27 May 2025
PUBLISHED 13 June 2025

CITATION
Xie J, Bai P, Xu X, Xie L, Li M and Gao Y (2025) Estimating the summer residual flow based on sea surface temperature within a narrow strait. *Front. Mar. Sci.* 12:1621833. doi: 10.3389/fmars.2025.1621833

Estimating the summer residual flow based on sea surface temperature within a narrow strait

Juncheng Xie[1], Peng Bai[1]*, Xiaowei Xu[2], Lingling Xie[3], Mingming Li[3]* and Ying Gao[1]

[1]Marine Science and Technology College, Zhejiang Ocean University, Zhoushan, China, [2]Zhoushan Natural Resource Surveying and Mapping Design Center, Zhoushan Natural Resources and Planning Bureau, Zhoushan, China, [3]College of Ocean and Meteorology, Guangdong Ocean University, Zhanjiang, China

Residual flow in straits manifests the interactions of multiple dynamic processes and serves as pivotal connectors between these processes, playing a crucial role in marine material-energy transport and ecosystem evolution. Current research predominantly relies on *in-situ* measurements and numerical modeling, yet both approaches incur high costs and struggle to obtain long-term residual current datasets, constraining our understanding of marine environments in straits and their adjacent basins. Addressing this gap, we developed an innovative algorithm to inversely calculate residual flow using satellite-derived sea surface temperature (SST) data, with a case study on the tide-dominated narrow Qiongzhou Strait in the northern South China Sea. Capitalizing on its distinctive summer SST pattern (eastern cooling vs. western warming) and prevailing westward residual current regime, we demonstrated that the thermal structure can be effectively characterized by a 1D balance equation incorporating temporal variation, horizontal advection, diffusion, and thermal forcing terms. Applying this framework to MODIS SST data (2003–2022), we reliably estimated summer residual flow velocities and fluxes over two decades. The analysis further revealed significant interannual variability in westward flow intensity, modulated by large-scale air-sea interactions: cyclonic wind anomalies over the northwestern South China Sea enhance westward currents, while anticyclonic anomalies induce weakening. This approach provides a cost-effective paradigm for monitoring long-term strait dynamics.

KEYWORDS

residual flow, sea surface temperature, upwelling, MODIS, Qiongzhou Strait

1 Introduction

A strait, defined as a narrow waterway connecting two seas or oceans between adjacent landmasses, serves not only as a critical maritime corridor and shipping hub with strategic military importance but also plays a pivotal role in global oceanographic processes. As crucial conduits linking distinct marine basins, straits regulate regional and even global thermohaline transport and material cycling through their complex water exchange patterns, circulation structures, and energy transfer mechanisms. For instance, the Mediterranean Overflow via the Gibraltar Strait significantly influences the Atlantic Meridional Overturning Circulation (Hernández-Molina et al., 2014; Swingedouw et al., 2019), while water exchange through the Bering Strait governs the physico-chemical and biological environments of both the Arctic and North Pacific Oceans (Woodgate et al., 2005; Grebmeier et al., 2006; Woodgate et al., 2012). Even in smaller-scale systems like the Qiongzhou Strait, intense tidal currents directly shape the unique "butterfly delta" submarine geomorphology at its eastern and western outlets (Ni et al., 2014).

Residual flow refers to the time-averaged, non-tidal components of oceanic flow that persist after filtering out high-frequency motions such as tides, inertial oscillations, and wind-driven surface waves. Residual flow in straits, emerging as net water transport from the interplay of multiple dynamic processes, serve as both a manifestation of complex hydrodynamic interactions and a key linkage connecting various oceanographic processes. The spatiotemporal characteristics of residual flow fundamentally control suspended particulate transport pathways, pollutant dispersion ranges, and nutrient cycling efficiency within straits. In strongly tidal straits, residual flow dominates the formation of sediment "trapping zones" through long-term cumulative effects, thereby modifying submarine topography and posing navigational challenges (Van Maren and Gerritsen, 2012; Ni et al., 2014; Ai et al., 2024). Notably, the Taiwan Strait acts as a conduit for wintertime transport of East China Sea water masses to the northeastern South China Sea under northeast monsoon forcing, significantly impacting local marine environments (Chen et al., 2020; Li et al., 2024) and consequently influencing fishery resource distribution patterns. These mechanisms underscore the irreplaceable scientific value of studying residual currents in straits for understanding marine material transport, ecosystem stability, and anthropogenic impacts.

The Qiongzhou Strait, situated between the Leizhou Peninsula of Guangdong Province and Hainan Island, China (Figure 1a), serves as the sole natural conduit for water exchange between the northern South China Sea and the Beibu Gulf, and ranks among China's three major straits. This east-west oriented strait extends approximately 80 km in length, with a minimum width of 19.4 km, averaging 44 m in water depth and reaching a maximum depth of 114 m. A 33-km-long tidal channel with water depths exceeding 60 m dominates the central strait, exhibiting asymmetric topography across its northern and southern flanks: the northern flank is relatively gentle whereas the southern side is steeper. During summer, the Qiongzhou Strait is dominated by the southerly monsoon (Figure 1b). Distinct thermal regimes characterize its eastern and western entrances: cold waters occupy the eastern entrance due to the development of coastal upwelling, while the western entrance is governed by vertically well-mixed warm waters resulting from intense tidal mixing combined with strong solar radiation (Figure 1b; Hu et al., 2003; Bai et al., 2016; Lin et al., 2016; Bai et al., 2020a, 2022).

The Qiongzhou Strait is a strong tide-dominated channel. Within the strait, diurnal tidal constituents predominantly propagate east to west. At the western entrance, the amplitude of diurnal tides ($\frac{O_1+K_1}{2}$) reaches 70 cm, gradually decreasing eastward to 25 cm at the eastern entrance. The maximum phase lag occurs in the southwestern strait (with minimal phase lags at both entrances), where tidal waves from both ends interact. The phase speed of westward-propagating diurnal tides measures approximately 10 m/s, significantly faster than eastward-propagating diurnal constituents. In contrast, the semidiurnal M_2 constituent propagates exclusively west-to-east from the Beibu Gulf, with its amplitude increasing from 20 cm at the western entrance to 40 cm at the eastern entrance. The phase lag difference between the strait's two ends is approximately 100° (equivalent to 6.5 hours), yielding a propagation speed of ~4.7 m/s, slower than diurnal tidal speeds. Both diurnal and semidiurnal tidal current ellipses align nearly parallel to the strait's axis. Diurnal tidal currents peak in the 5–10 m water layer, exhibiting amplitudes of ~30 cm/s at the western entrance and up to 100 cm/s at the eastern entrance. Notably, near-bottom currents (within 3 m of the seabed) maintain substantial amplitudes of 30–50 cm/s. The M_2 semidiurnal currents display weaker intensities (10–20 cm/s), approximately one order of magnitude smaller than diurnal currents. Unlike diurnal constituents, semidiurnal currents show minimal vertical variability, with near-identical surface and near-bed current magnitudes (Shi et al., 2002; Chen et al., 2009; Zheng et al., 2024).

In coastal shallow seas, waves alongside tides are key hydrodynamic drivers (e.g., Gao et al., 2017, 2021, 2023, 2024). During summer, the southwest monsoon weakens as it encounters Hainan Island (Figure 1b), resulting in mild wind waves with disorganized directional distribution in Qiongzhou Strait. In contrast, the northeast winter monsoon directly impacts the strait. Waves from the open sea east of the strait also propagate unimpeded into the region, generating larger waves (~1 m height). Strong tidal currents in the strait further modulate wave dynamics. Current-induced convergence and wavenumber shifts can amplify significant wave height at the strait's eastern entrance. Additionally, tidal flow regulates peak wave directions through current-induced refraction (Bai et al., 2020b).

The southwest monsoon governs the entire northwestern South China Sea, leading to the early assumption that summer water transport from the Beibu Gulf through the Qiongzhou Strait to the eastern shelf seas of the Leizhou Peninsula would generate eastward residual flow within the strait. However, Shi et al. (2002) demonstrated, using 37-year observational datasets of tidal elevation and currents combined with numerical modeling, that a persistent westward residual flow (10–40 cm/s) exists year-round in the strait. This flow contributes a summer water transport of 0.1–0.2 Sv into the Beibu Gulf. Subsequently, Yang et al. (2003) identified

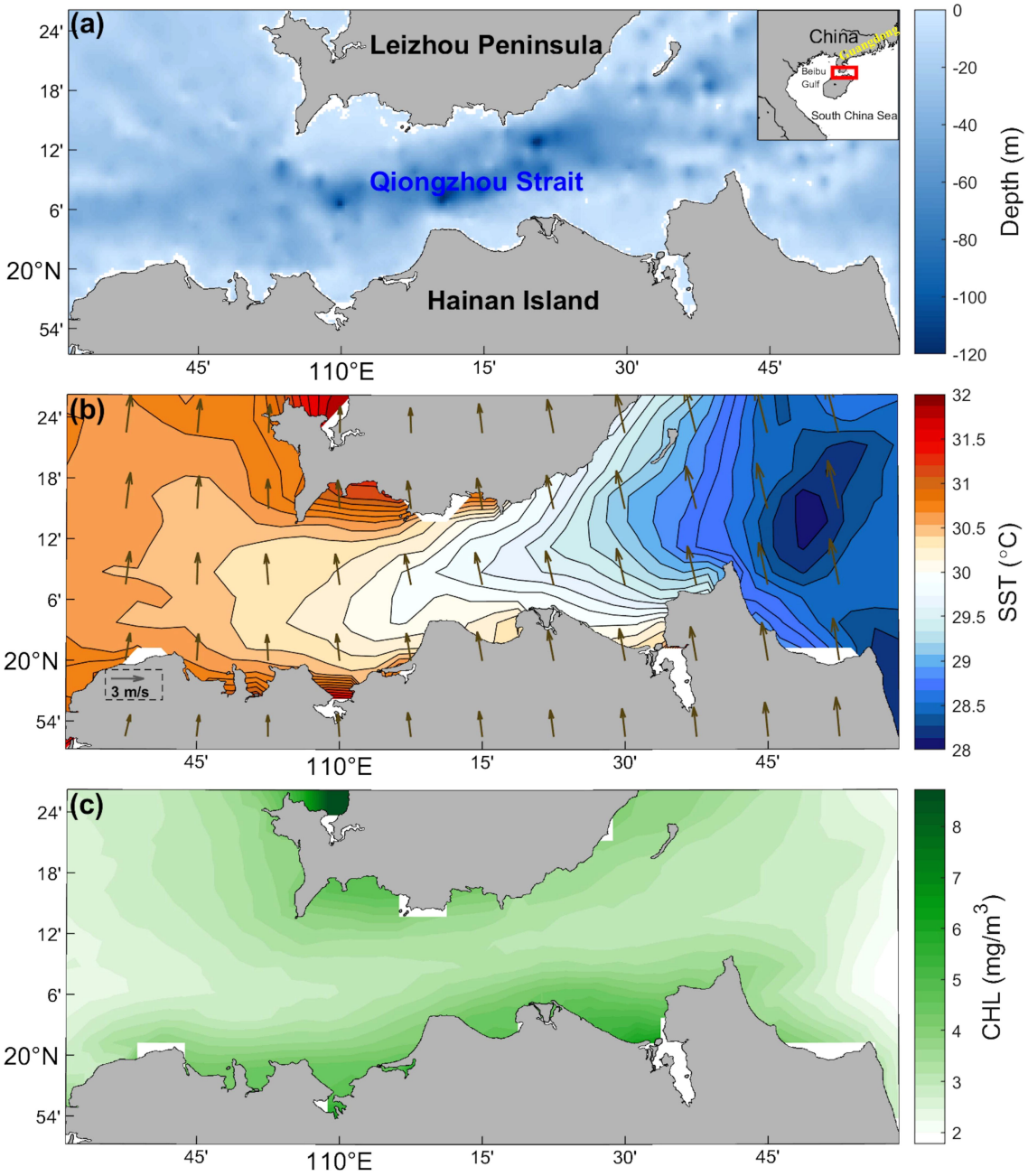

FIGURE 1
(a) Geographical setting and bathymetric distribution of the Qiongzhou Strait; **(b)** Climatological summer SST and wind vector field distribution in the Qiongzhou Strait; **(c)** Climatological summer sea surface chlorophyll-a (Chl-a) concentration distribution in the Qiongzhou Strait.

westward residual flow structures in the Qiongzhou Strait during summer using drifter bottle data. Employing a three-dimensional ECOM model, Chen et al. (2009) systematically investigated tidal-induced residual flow, wind-driven currents, and density-driven circulation. Their results confirmed that westward residual flow dominates the strait in both winter and summer, with tidal rectification generating westward residual currents of 5–30 cm/s. These currents fully suppress wind-driven eastward flows (5–15 cm/s), establishing tidal dynamics as the primary driver of the strait's westward residual flow. Wang et al. (2014) analyzed summer Acoustic Doppler Current Profiler (ADCP) measurements, revealing meridional variability in the westward residual flow, with peak velocities reaching -0.34 m/s and a mean westward transport of 0.16 Sv. Recently, Zheng et al. (2024) implemented the SCHISM model to further elucidate residual flow dynamics in the Qiongzhou Strait. Their study quantified a mean summer westward residual flow of 0.2 m/s and identified that wind stress curl differences between the eastern and western strait entrances can induce transient eastward residual flows. According to Shi et al. (2002), summer westward transport through the Qiongzhou Strait

accounts for approximately 44% of the Beibu Gulf's water renewal. A series of studies (Wu et al., 2008; Ding et al., 2017; Yang et al., 2020; Zavala-Garay et al., 2022) have confirmed that this transport mechanism critically governs the formation of summer cyclonic circulation within the Beibu Gulf. Additionally, the summer westward residual flow significantly modulates thermal patterns at the western strait entrance (Bai et al., 2022) and influences seabed geomorphology and sediment deposition (Ni et al., 2014).

Current research methodologies for investigating residual flow in the Qiongzhou Strait primarily rely on two approaches: *in situ* data analysis and ocean numerical modeling (Shi et al., 2002; Yang et al., 2003; Chen et al., 2007; Yan et al., 2008; Chen et al., 2009; Wang et al., 2014; Zhu et al., 2014, 2015; Zavala-Garay et al., 2022; Zheng et al., 2024; Chen et al., 2025). However, both methodologies demand substantial human, material, and temporal resources while yielding limited long-term residual flow records. This constraint has directly contributed to significant discrepancies in residual flow intensity reported in previous studies focusing on different summer periods within the strait. To address these limitations, this study proposes an innovative algorithm for residual flow inversion based on the unique east-west thermal contrast (cooler eastern vs. warmer western sectors) and westward residual flow background during summer seasons. By solving a one-dimensional thermal balance equation using MODIS-derived sea surface temperature (SST) data, we achieved cost-effective and physically reasonable estimations of summer residual flow patterns in the Qiongzhou Strait from 2003 to 2022. The remainder of this paper is organized as follows: Section 2 describes the primary datasets employed in this study. Section 3 details the residual flow inversion algorithm derived from SST observations. Section 4 presents the estimated summer residual flow patterns and evaluates the reliability of the proposed methodology. Section 5 investigates the interannual variability mechanisms through selected representative years. Section 6 concludes with a summary of key findings and implications.

2 Data

2.1 Remote-sensed SST

Satellite-derived SST has emerged as a critical observational tool for oceanic studies, providing essential insights into diverse marine phenomena including marine heatwaves, ecosystem dynamics, frontal processes, mesoscale eddies, typhoon-ocean interactions, and air-sea exchange mechanisms. For residual flow quantification in the Qiongzhou Strait, we utilized the Moderate Resolution Imaging Spectroradiometer (MODIS) Level 3 SST product (2003–2022 summer months) obtained from NASA Ocean Color Platform (http://oceancolor.gsfc.nasa.gov/). This dataset contains observations from both Aqua (MODIS-A) and Terra (MODIS-T) satellite platforms, offering 4 km spatial resolution gridded data through optimal spatiotemporal compositing algorithms.

2.2 Chl-a data

The summer climatology (June–August) of monthly chlorophyll-a (Chl-a) concentration, obtained from the NASA Ocean Color database (https://oceancolor.gsfc.nasa.gov/), was employed to determine Jerlov water types (Jerlov, 1968) in the Qiongzhou Strait. The MODIS-derived Chl-a dataset, with a spatial resolution of 4 km, demonstrated sufficient sensitivity to resolve the spatiotemporal Chl-a distribution patterns characteristic of this semi-enclosed Qiongzhou Strait.

2.3 Satellite-observed winds

The Cross-Calibrated Multi-Platform (CCMP) Level-4 wind vector product was employed to characterize the atmospheric dynamic forcing in the study region. This advanced dataset synthesizes microwave sensor-derived ocean surface wind observations (10 m elevation) with ECMWF reanalysis background fields through variational assimilation, providing gap-free spatial continuity at 0.25° × 0.25° gridding with six-hour temporal resolution. The CCMP product can be obtained from the Remote Sensing Systems website (http://www.remss.com/ccmp/).

2.4 Reanalyzed air-sea heat fluxes

The ERA5 reanalysis dataset was utilized to quantify surface net heat flux and shortwave radiation through comprehensive air-sea heat flux components. This state-of-the-art reanalysis integrates multi-source observations (satellites, meteorological stations, ships, and buoys) with advanced numerical weather prediction simulations via 4D-Var data assimilation, delivering continuous meteorological records at 0.25° × 0.25° spatial resolution. Recognized for its high assimilation quality and comprehensive physical parameterization, ERA5 has been extensively utilized in climate-ocean interaction studies, particularly for resolving energy budget dynamics and extreme meteorological events.

2.5 Reanalyzed circulation data

To validate the interannual variability of residual flow derived in this study, the GLORYS12V1 reanalysis product from the Copernicus Marine Environment Monitoring Service (CMEMS) (https://marine.copernicus.eu/access-data) was employed. This dataset provides global three-dimensional fields of seawater temperature, salinity, and current velocities since 1993, featuring a horizontal resolution of 1/12° with 50 vertical layers that adequately resolve the Qiongzhou Strait's bathymetry. Developed on the NEMO ocean modeling platform, the product enhances accuracy through multivariate data assimilation techniques

including reduced-order Kalman filtering and 3D-var analysis, and has been extensively adopted in global marine science research.

It should be noted that while this product cannot accurately represent tidally-induced residual flow (i.e., net residual flow) due to the exclusion of tidal forcing, it effectively captures wind-driven residual flow and baroclinic-effect-induced residual flow. Given that tidal adjustment contributions to residual flow remain relatively invariant interannually at seasonal scales, the GLORYS12V1 product demonstrates sufficient capability to characterize interannual variations of residual flow in the strait, despite its limitations in quantifying absolute residual flow magnitudes.

3 Residual flow retrieval algorithm

3.1 One-dimensional thermal balance equation for the strait

Figure 1b depicts the climatological summer SST and wind field distribution in the Qiongzhou Strait. The eastern strait is dominated by cold water masses originating from the northeastern Hainan upwelling system (Bai et al., 2016, 2020a, 2022; Lin et al., 2016), while the western strait exhibits elevated SST due to strong tidal mixing synergized with intense solar radiation (Hu et al., 2003; Bai et al., 2022). Persistent westward residual flow, as consistently reported in previous studies, facilitates the westward transport of cold water from the eastern strait, generating a characteristic westward-protruding SST tongue structure (Figure 1b). The study area experiences substantial net heat flux in the upper ocean during summer, compounded by the strait's unique east-west oriented narrow topography.

Integrating these dynamic, thermodynamic, and bathymetric factors, Figure 2a schematically illustrates the summer SST pattern, net surface heat flux distribution, and residual flow configuration. The narrow geometry permits simplification of the upper mixed layer thermal balance equation to a one-dimensional formulation expressed as (Qu, 2003; Liang and Wu, 2013; Wang et al., 2023; Zhang et al., 2023):

$$\frac{\partial T}{\partial t} + U_{residual}\frac{\partial T}{\partial x} = \frac{Q - Q_d}{h\rho C_p} + a\frac{\partial^2 T}{\partial x^2} \tag{1}$$

where T is the temperature in the surface mixed layer, t is time, x is the east-west coordinate, $U_{residual}$ is the residual flow within the strait, Q is the sum of air-sea heat fluxes, including shortwave radiation, longwave radiation, sensible heat flux, and latent heat flux, Q_d is the shortwave radiation penetrating below the mixed layer, h is the mixed layer depth, $\rho = 1022.0\ \mathrm{kg/m^3}$ is the seawater density, $C_p = 4002.6\ \mathrm{J/kg \cdot °C}$ is the specific heat capacity of seawater, $a = \frac{k}{\rho C_p}$ is the heat transfer coefficient of seawater and $k = 0.616\ \mathrm{W/m \cdot °C}$ is the coefficient of seawater thermal conductivity. Notably, (Equation 1) should theoretically contain an additional residual term on its right-hand side, primarily consisting of vertical entrainment and mixing processes. However, given its relatively minor magnitude compared to dominant terms and for numerical tractability, this term has been systematically neglected in our formulation. Consequently, the simplified one-dimensional

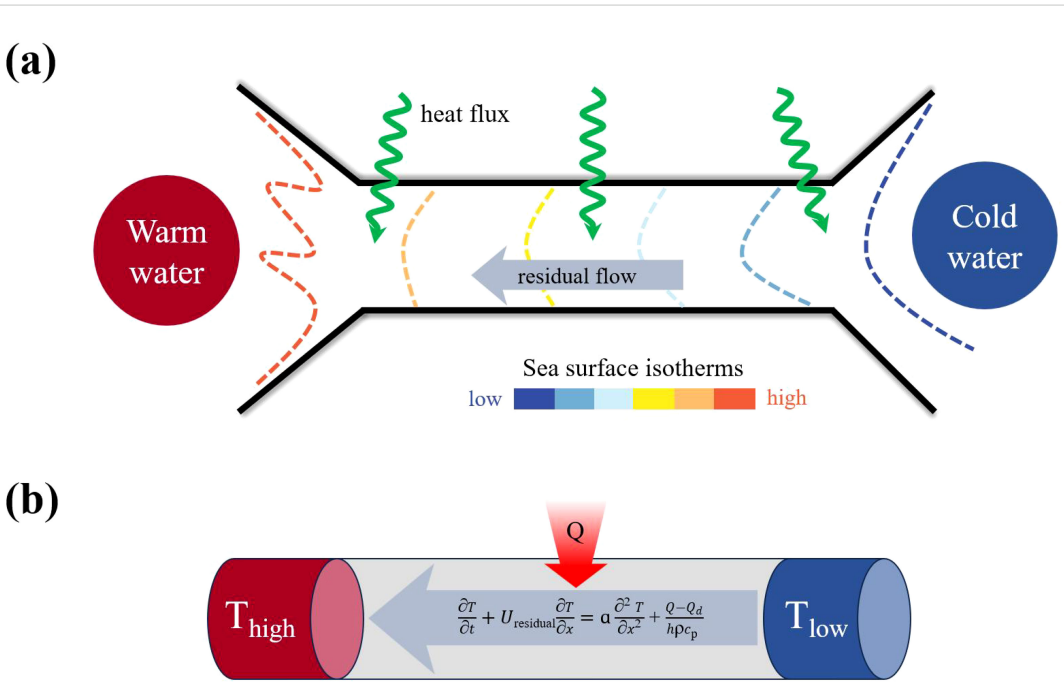

FIGURE 2
(a) Schematic of summer SST, net surface heat flux, and residual flow patterns in the Qiongzhou Strait; **(b)** 1-D simplified thermal model with governing equation for summertime Qiongzhou Strait.

thermal balance model governing summer sea surface temperature variations in the Qiongzhou Strait, along with its control equations, can be mathematically expressed as shown in Figure 2b.

3.2 Discretization of the 1D thermal balance equation

Equation 1 governs the thermal dynamics within the strait, incorporating four principal components: the temporal variation term, advection term, horizontal diffusion term, and heat source term. Specifically, the advection term arises from the westward transport of cold water mass by residual flow. Through Forward Time Central Space (FTCS) discretization, the numerical formulation of Equation 1 becomes:

$$T_i^{j+1} = T_i^j + a \cdot \frac{\Delta t}{\Delta x^2} \cdot (T_{i+1}^j - 2T_i^j + T_{i-1}^j) - U_{residual} \cdot \frac{\Delta t}{\Delta x} \cdot (T_{i+1}^j - T_i^j) + \Delta t \cdot \frac{Q - Q_d}{h\rho C_p} \quad (2)$$

where $i = 1, 2, 3 \cdots, I-1$, I denotes the discrete spatial grid points along the x-axis, $j = 1, 2, 3 \cdots, J-1$, J represents the discrete time layers, $\Delta t = 60$ s is the temporal step size, and $\Delta x = 2100$ mis the spatial step size. The question then arises: how should the boundary and initial conditions for T be established? This study selects a control line AB along the west-east central axis of the strait (Figure 3a), utilizing the SST distribution along this transect to inversely calculate the westward residual flow. This approach effectively eliminates interference from meridional dynamic and thermodynamic processes on SST variations. For boundary conditions, we set $T_{i=1} = T_A$, $T_{i=I} = T_B$, where T_A and T_B correspond to the SST values at the western (left) and eastern (right) endpoints of control line AB, respectively, obtainable from MODIS SST. Regarding initial conditions, given the observed east-to-west thermal gradient within the strait (Figure 1b), this study adopts the formulation $T^{j=1}_{i\in[2,\,I-1]} = T_B$.

Figure 3b displays the climatological SST distribution along control line AB during summer, revealing a quasi-linear increasing pattern from the eastern to the western strait. This thermal profile aligns with the temperature distribution constrained by the one-

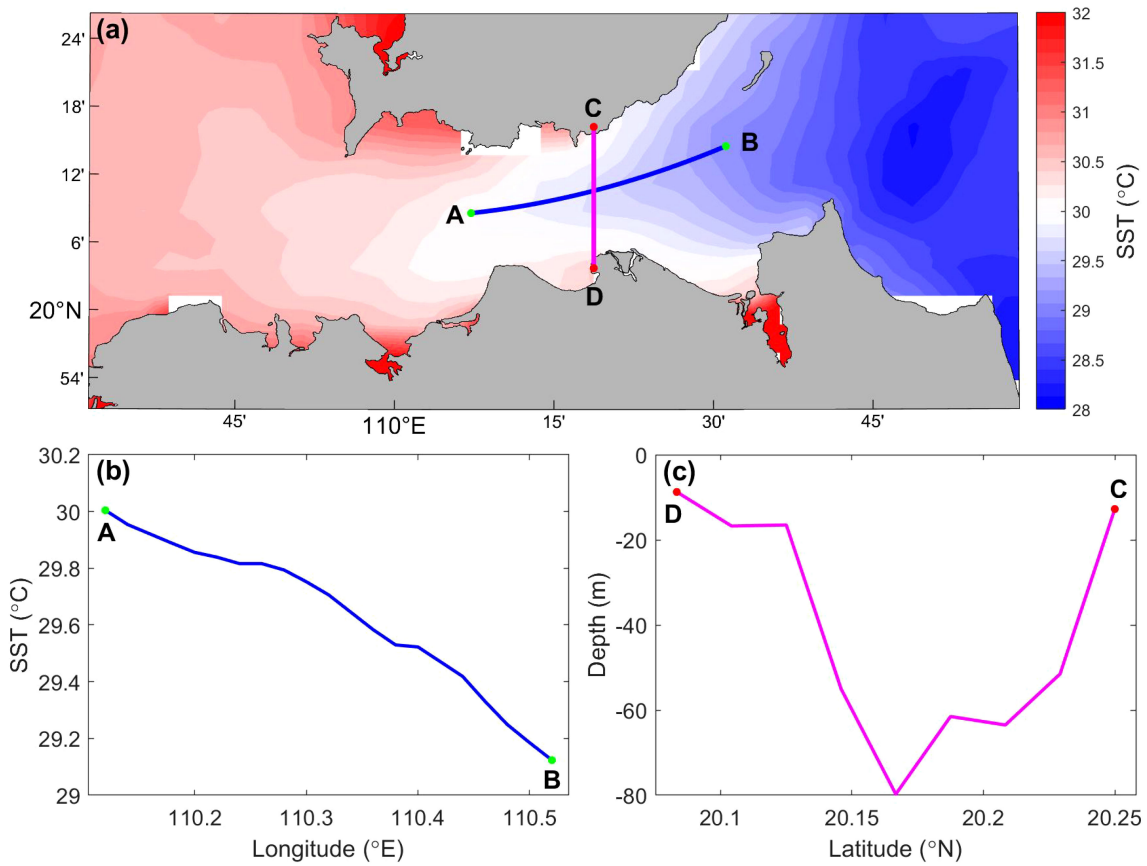

FIGURE 3
(a) Locations of SST used for inverse calculation of the westward residual flow (control line AB); **(b)** Summer climatological SST distribution along control line AB; **(c)** Bathymetric distribution along control line CD employed for computing westward transport.

dimensional simplified governing equation presented in (Equation 1), thereby validating the inverse calculation method for residual flow within the strait under this theoretical framework. Simultaneously, the control line CD was designated as the volumetric flux calculation transect (Figure 3a), with its bathymetric profile shown in Figure 3c. For computational purposes, we assumed uniform residual flow distribution across the entire CD cross-section during flux calculations.

3.3 Key parameters

A critical question arises: how should the mixed layer thickness h in the heat flux forcing term be appropriately determined? Figure 4 displays the vertical temperature profiles measured at stations S1–S5 in the eastern Qiongzhou Strait during July 2018. These observations reveal a shallow summer mixed layer (~5 m) in the study area, with increasingly uniform vertical thermal stratification at stations closer to the strait interior (S4, S5). Consequently, we select the upper 5 m water column (h=5 m) to calculate the net surface heat flux contribution to seawater heating within this layer.

To determine the net heat flux absorbed by the upper 5 m layer, it is essential to account for the residual shortwave radiation Q_d penetrating to 5 m depth. Figure 1c illustrates the climatological summer sea surface Chl-a concentration distribution in the Qiongzhou Strait, showing central strait values of 2–3 mg/m³. Based on the empirical relationship between Jerlov water types and Chl-a concentrations (Morel, 1988) and results from Zavala-Garay et al. (2022), the water type along the central axis corresponds to intermediate Jerlov II–III classifications. Further calculations of Q_d employ the shortwave radiation attenuation coefficients for different Jerlov water types as defined by Paulson and Simpson (1977).

With all terms except the residual flow $U_{residual}$ in the one-dimensional SST control (Equation 2) now constrained by observational and theoretical constraints (Equation 2), we implement an inversion workflow: (1) prescribe westward residual flow velocities using a test range of $U_{residual} \in [0.0, -0.5]$ with a -0.005 m/s increments. (2) generate numerical SST solutions along control line AB for each velocity value. (3) identify the velocity corresponding to the optimal solution of SST along control line AB as the magnitude of residual flow. This approach yields the climatological (or annual) summer westward residual flow speed.

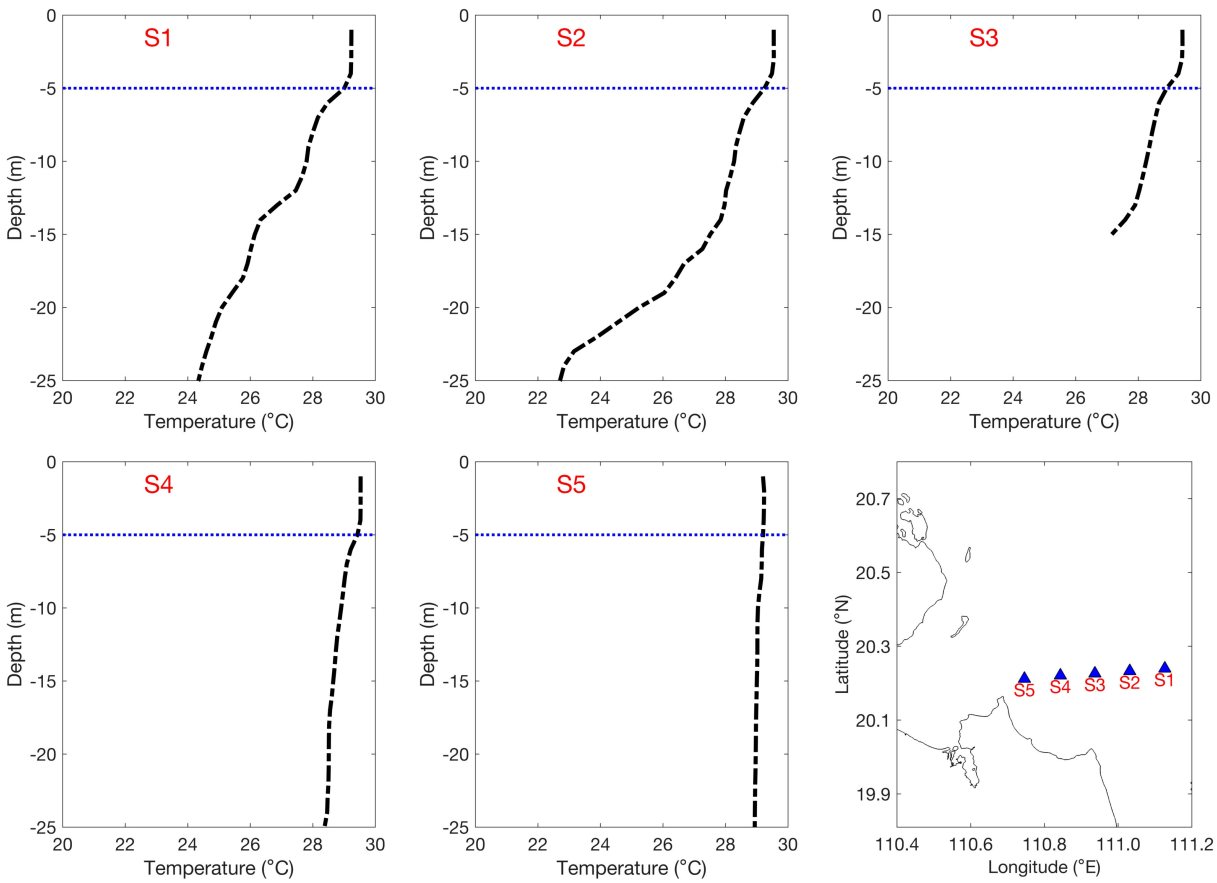

FIGURE 4
Vertical distributions of shipboard-measured sea temperature at stations S1–S5 in the eastern Qiongzhou Strait during summer, with station locations illustrated in the lower right panel.

4 Residual flow and flux in 2003–2022

The summer climatological residual current for 2003–2022 in the Qiongzhou Strait was estimated using the aforementioned inverse calculation methodology. Figure 5 presents a comparative analysis between MODIS satellite-derived SST measurements (red line) and the optimal simulated SST distribution (thick blue dashed line) along control line AB. The optimal calculated SST demonstrates good agreement with the observed SST pattern along control line AB. The corresponding residual current $U_{residual}$ = −0.130 m/s (negative values indicate westward direction) derived from this optimal SST solution drives a water transport of approximately 0.1102 Sv from the Qiongzhou Strait into the Beibu Gulf. This finding aligns with prior research documenting summer residual currents of 0.05–0.3 m/s (equivalent to 0.026–0.2 Sv transport) in the Qiongzhou Strait (Table 1), thereby validating the reasonableness of our results.

Furthermore, summer westward residual flow in the Qiongzhou Strait during 2003–2022 was estimated using MODIS SST. Figure 6 compares the MODIS-observed summer SST (solid red lines) with the optimal simulated SST (blue dashed lines) along control line AB for individual years. The results reveal that most years exhibit a linear east-to-west increasing SST pattern along control line AB. Meanwhile, the optimally inverted SST generally aligns well with MODIS observations across most years, which further validates the rationality of both the one-dimensional thermal balance (Equation 1) developed in this study and the residual flow inversion methodology. Notably, the thermal control line in the summer 2010 appears shorter than in other years due to missing MODIS SST data in that specific period.

Building upon these findings, Figure 7 quantitatively illustrates the temporal distribution of summer residual flow and associated volume transport in the Qiongzhou Strait from 2003 to 2022. The results reveal pronounced interannual variability in both residual current intensity and transport magnitude, aligning with the numerical simulations of Zheng et al. (2024), which suggest that interannual variability in local winds could lead to potential fluctuations in the intensity of summer residual currents. During the study period, the maximum westward residual flow occurred in 2018, recording values of -0.5040 m/s (velocity) and 0.4271 Sv (transport). In contrast, the minimum westward flow was observed in 2016, with corresponding estimations of -0.0640 m/s and 0.0542 Sv, respectively.

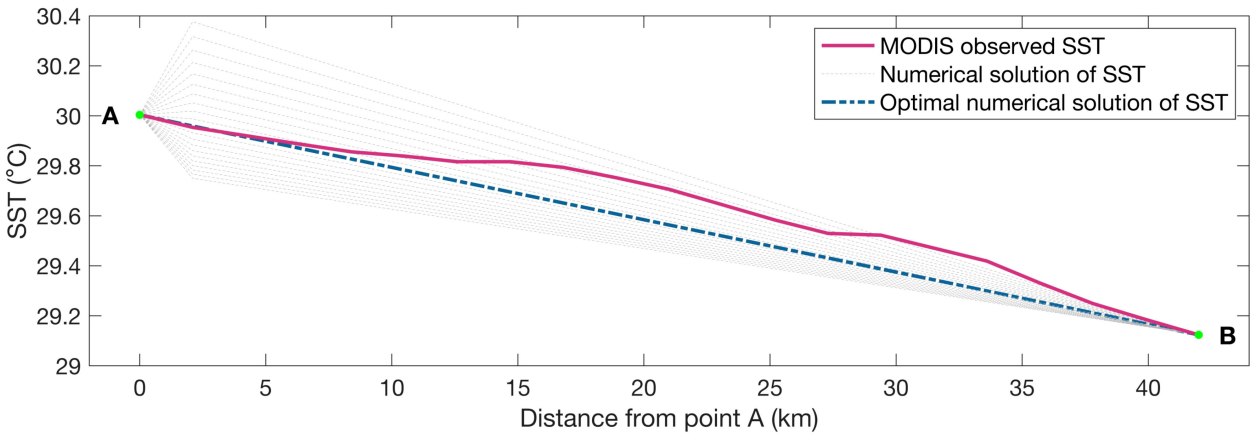

FIGURE 5
Modeled SST distributions along control line AB under different westward residual current scenarios (gray dashed lines); the red solid line represents the MODIS-observed summer climatological SST along control line AB, while the blue dashed line indicates the optimal simulated SST.

TABLE 1 Previous studies on residual flow and flux in Qiongzhou Strait.

Reference	Westward residual current velocity (m/s)				Westward volume transport (Sv)				Method
	winter	spring	summer	autumn	winter	spring	summer	autumn	
Shi et al. (2002)	0.2–0.4		0.1–0.3		0.2–0.4		0.1–0.2		Observation analysis
Chen et al. (2009)	0.05–0.4	/	0.05–0.3	/	0.116	/	0.026	/	ECOM simulation
Wang et al. (2014)			0.34				0.16		Observation analysis
Zheng et al. (2024)	0.4–0.5	/	0.2	/	/	/	/	/	SCHISM simulation

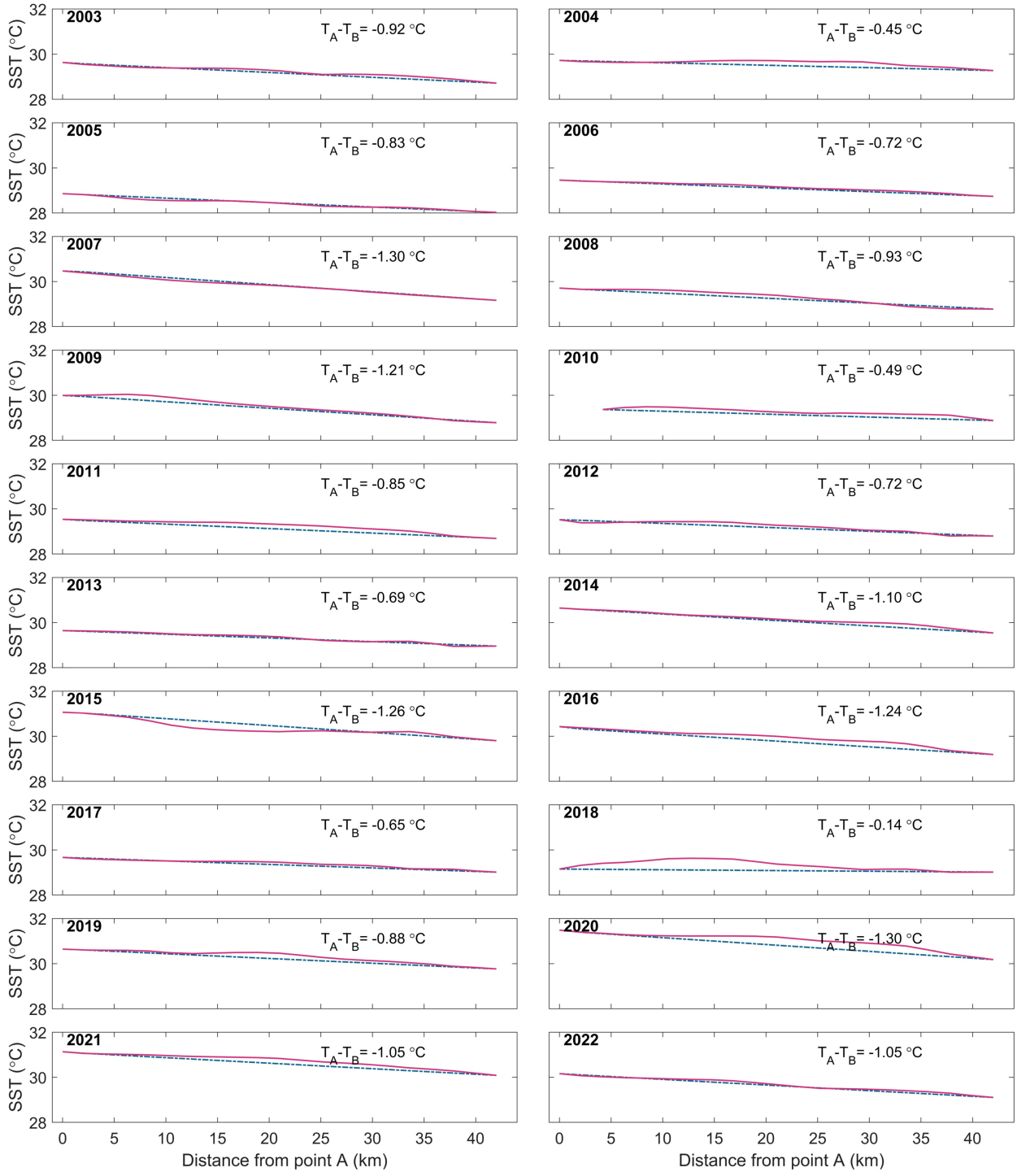

FIGURE 6
Comparison of MODIS-observed summer SST (red solid line) and the optimal simulated SST (blue dashed line) along control line AB during 2003–2022.

5 Discussion

Figure 7 demonstrates that the summer westward residual flow velocities in the Qiongzhou Strait during 2004, 2010, and 2018 consistently exceeded 0.3 m/s, significantly surpassing the maximum westward residual currents previously reported based on field measurements or three-dimensional circulation models (Shi et al., 2002; Chen et al., 2009; Zheng et al., 2024). Does this imply that our original SST-based inversion method for residual flow is unreliable?

The summer residual flow in the Qiongzhou Strait primarily comprises three components: (1) residual flow induced by tidal

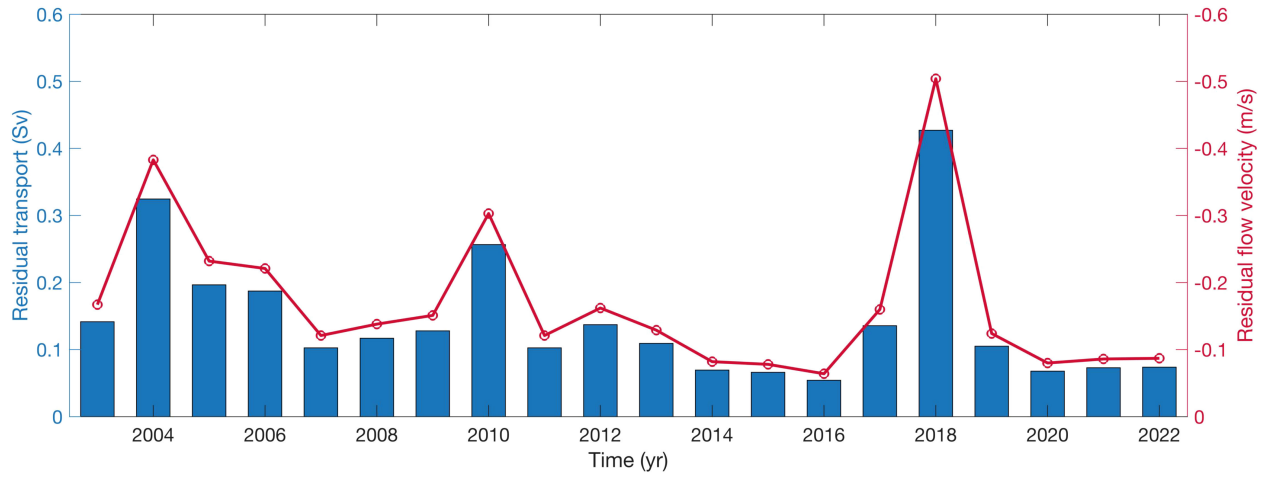

FIGURE 7
Temporal evolution of summer residual flow and residual transport in the Qiongzhou Strait from 2003 to 2022.

rectification over complex topography, (2) wind-driven residual currents, and (3) baroclinic-effect-driven residual currents caused by density gradients (Shi et al., 2002; Chen et al., 2009; Zhu et al., 2014, 2015; Zheng et al., 2024). On seasonal timescales, residual flow forced by tidal rectification remains relatively constant across years. Therefore, interannual variability in the strait's residual flow is predominantly governed by wind-driven and baroclinic-effect-driven components. This variability can be validated using the GLORYS12V1 reanalysis product, which corroborates the interannual trends in our inverted residual flow.

Figure 8 illustrates the spatial distributions of summer wind anomalies and associated current anomalies in the northwestern South China Sea during 2004, 2010, and 2018. Cyclonic wind anomalies were observed in all three years, which intensified the western Guangdong coastal current. This enhanced flow transported additional water masses from the western Guangdong shelf into the Qiongzhou Strait, where they merged with the westward residual flow and entered the Beibu Gulf. This mechanism coherently explains the anomalously strong westward residual flow in the strait during these years and further validates the reliability of our inversion method. The wind field over the South China Sea exhibits high sensitivity to large-scale air-sea interactions. Previous studies have extensively documented and elucidated the linkage between South China Sea wind anomalies and ENSO events (e.g., Du et al., 2009, 2011; Xie et al., 2009, 2010; Chowdary et al., 2011; Jing et al., 2011). For instance, during the strong El Niño summer of 2015, pronounced anticyclonic wind anomalies occurred in the northwestern South China Sea. These anomalies strengthened wind-driven eastward residual currents in the strait (not shown), substantially offsetting the westward residual flow generated by tidal rectification. Consequently, the net residual flow in the strait weakened markedly, with westward residual velocities dropping to the lowest levels observed during the study period (Figure 7). Note that, prior studies (e.g., Zheng et al., 2024; Chen et al., 2025) also highlighted that wind stress curl modulates residual flow intensity in the strait by altering the sea surface height gradient between its eastern and western ends. In summary, our SST-based inversion method for estimating residual flow in the Qiongzhou Strait is both physically sound and robust, yielding credible results.

6 Conclusions

The Qiongzhou Strait serves as the sole west-east conduit connecting the northern South China Sea shelf and the Beibu Gulf. During summer, westward water transport through the strait contributes approximately half of the Beibu Gulf's water renewal volume. This mass exchange plays a decisive role in shaping the summer cyclonic circulation within the Beibu Gulf (e.g., Wu et al., 2008; Zavala-Garay et al., 2022) while modulating key processes including thermal patterns, submarine geomorphology, sediment transport, nutrient fluxes, and ecological dynamics in both the strait and the gulf (e.g., Ni et al., 2014; Bai et al., 2022; Lao et al., 2022; Geng et al., 2024).

Nevertheless, current investigations into residual flow in the Qiongzhou Strait remain constrained to two conventional approaches: *in-situ* observational analysis and numerical ocean modeling. Both methodologies demand substantial human, material, and temporal investments, yet fail to provide long-term residual current datasets. These limitations impede a comprehensive understanding of strait dynamics and broader marine environmental processes in the northwestern South China Sea.

To address these challenges, this study pioneers an innovative algorithm that inversely calculates summer residual flow within the strait using satellite-derived SST data. The algorithm capitalizes on two critical factors: the unique east-west thermal gradient (cooler eastern vs. warmer western sectors) across the strait during

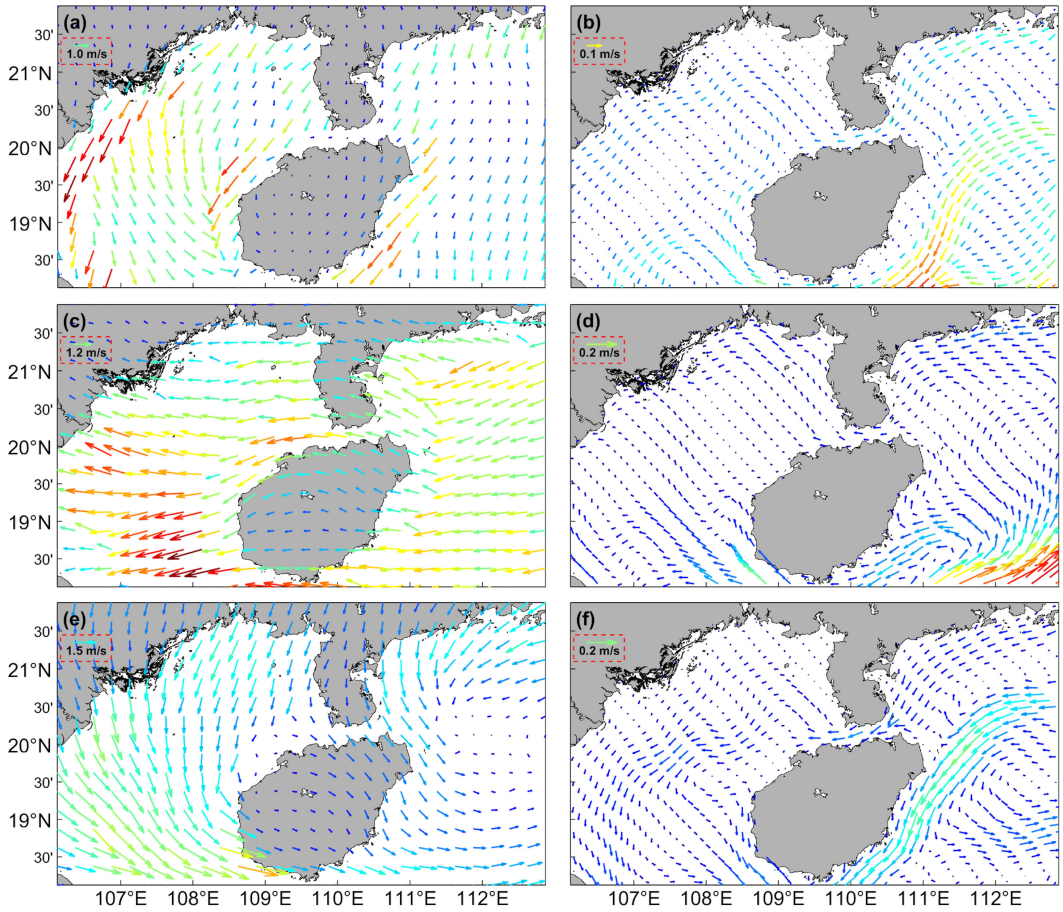

FIGURE 8
Anomaly spatial patterns of summer wind field **(a)** and current field **(b)** in the northwestern South China Sea in 2004; **(c-f)** present the corresponding scenarios for 2010 and 2018, respectively.

summer, and the persistent westward residual flow regime. Principal findings are summarized as follows:

1. The summer SST pattern in the Qiongzhou Strait can be effectively characterized using a one-dimensional thermal balance equation incorporating the temporal tendency term, horizontal advection term, horizontal diffusion term, and thermal forcing term.
2. A robust estimation of residual flow and flux in the summer Qiongzhou Strait during the two-decade period (2003–2022) has been achieved through satellite-derived SST data, demonstrating the feasibility of remote sensing approaches for long-term hydrodynamic assessments.
3. Interannual variability in westward residual flow intensity was identified in the summer Qiongzhou Strait, modulated by large-scale air-sea interactions. Enhanced westward residual flow correlates with cyclonic wind anomalies over the northwestern South China Sea, whereas anticyclonic wind anomalies systematically suppress these currents.

It should be emphasized that the developed one-dimensional thermal balance equation for Qiongzhou Strait incorporates reasonable simplifications accounting for local bathymetry and summer dynamic/thermal conditions, particularly through the exclusion of vertical processes and meridional dynamic influences on SST evolution. Furthermore, our residual flux calculation assumes uniform cross-sectional distribution of the residual flow, despite documented spatial heterogeneity in both horizontal dimensions and vertical profiles (e.g., Shi et al., 2002; Chen et al., 2009; Zheng et al., 2024). While this methodological approach may introduce uncertainties in the current quantification, it does not fundamentally compromise the validity or practical utility of our inversion methodology for deriving residual flow from SST patterns. Future studies could adopt the methodological framework presented here to develop a vertically resolved two-dimensional thermal balance equation, thereby enhancing the precision of residual flow estimates.

Data availability statement

Publicly available datasets were analyzed in this study. The MODIS SST and Chl-a are acquired from NASA Ocean Color Web at https://oceancolor.gsfc.nasa.gov/; the CCMP wind vectors are available at Remote Sensing Systems following https://www.remss.

com/; the ERA5 reanalyzed air-sea heat fluxes are get from Copernicus Climate Data Store at https://cds.climate.copernicus.eu/; the GLORYS12V1 product are obtained from the Copernicus Marine Data Store at https://data.marine.copernicus.eu/products.

Author contributions

JX: Conceptualization, Writing – review & editing, Funding acquisition, Methodology, Formal analysis, Writing – original draft. PB: Visualization, Writing – original draft, Funding acquisition, Formal analysis, Conceptualization, Methodology, Investigation, Writing – review & editing. XX: Formal analysis, Writing – original draft. LX: Supervision, Writing – review & editing, Funding acquisition. ML: Data curation, Writing – review & editing, Formal analysis. YG: Investigation, Writing – original draft, Formal analysis, Validation.

Funding

The author(s) declare that financial support was received for the research and/or publication of this article. This study was jointly funded by the National Natural Science Foundation of China (Nos. 42106017, 42206004), the Zhejiang Provincial Natural Science Foundation of China (No. LMS25D060003), the Special Fund for Zhejiang Ocean University from Bureau of Science and Technology of Zhoushan (No. 2023C41006), and the Foundation of Guangdong Provincial Observation and Research Station for Tropical Ocean Environment in Western Coastal Waters (No. 2024B1212040008).

Conflict of interest

The authors declare that the research was conducted in the absence of any commercial or financial relationships that could be construed as a potential conflict of interest.

Generative AI statement

The author(s) declare that no Generative AI was used in the creation of this manuscript.

Publisher's note

References

Ai, L., Liu, S., Cong, S., Zhang, H., Cao, P., Wu, K., et al. (2024). Spatial variability of surface sediments in the Malacca strait and its implications for sedimentary environments. *J. Asian Earth Sci.* 259, 105922. doi: 10.1016/j.jseaes.2023.105922

Bai, P., Gu, Y., Li, P., and Wu, K. (2016). Modelling the upwelling off the east Hainan Island coast in summer 2010. *Chin. J. Oceanol. Limnol.* 34, 1358–1373. doi: 10.1007/s00343-016-5147-5

Bai, P., Ling, Z., Liu, C., Wu, J., and Xie, L. (2020b). Effects of tidal currents on winter wind waves in the Qiongzhou Strait: A numerical study. *Acta Oceanol. Sin.* 39, 33–43. doi: 10.1007/s13131-020-1673-2

Bai, P., Wang, J., Zhao, H., Li, B., Yang, J., Li, P., et al. (2022). Thermal structure of water exchange at the entrance of a tide-dominated strait. *Remote Sens.* 14, 3053. doi: 10.3390/rs14133053

Bai, P., Yang, J., Xie, L., Zhang, S., and Ling, Z. (2020a). Effect of topography on the cold water region in the east entrance area of Qiongzhou Strait. *Estuarine Coast. Shelf Sci.* 242, 106820. doi: 10.1016/j.ecss.2020.106820

Chen, C., Li, P., Shi, M., Zuo, J., Chen, M., and Sun, H. (2009). Numerical study of the tides and residual currents in the Qiongzhou Strait. *Chin. J. Oceanol. Limnol.* 27, 931–942. doi: 10.1007/s00343-009-9193-0

Chen, D., Lian, E., Shu, Y., Yang, S., Li, Y., Li, C., et al. (2020). Origin of the springtime South China Sea Warm Current in the southwestern Taiwan Strait: Evidence from seawater oxygen isotope. *Sci. China Earth Sci.* 63, 1564–1576. doi: 10.1007/s11430-019-9642-8

Chen, J. K., Xie, L. L., Li, J. Y., and Li, M. M. (2025). Spring water volume transport across the Qiongzhou Strait derived from mooring observations. *Adv. Mar. Sci.* 43, 1–17. doi: 10.12362/j.issn.1671-6647.20250108001

Chen, B., Yan, J. H., Wang, D. R., and Shi, M. C. (2007). The transport volume of water through the Qiongzhou Strait in the winter season. *Periodical Ocean Univ. China* 37, 357–364. doi: 10.16441/j.cnki.hdxb.2007.03.003

Chowdary, J. S., Xie, S. P., Luo, J. J., Hafner, J., Behera, S., Masumoto, Y., et al. (2011). Predictability of Northwest Pacific climate during summer and the role of the tropical Indian Ocean. *Climate Dynamics* 36, 607–621. doi: 10.1007/s00382-009-0686-5

Ding, Y., Bao, X., Yao, Z., Zhang, C., Wan, K., Bao, M., et al. (2017). A modeling study of the characteristics and mechanism of the westward coastal current during summer in the northwestern South China Sea. *Ocean Sci. J.* 52, 11–30. doi: 10.1007/s12601-017-0011-x

Du, Y., Xie, S. P., Huang, G., and Hu, K. (2009). Role of air–sea interaction in the long persistence of El Niño–induced north Indian Ocean warming. *J. Climate* 22, 2023–2038. doi: 10.1175/2008JCLI2590.1

Du, Y., Yang, L., and Xie, S. P. (2011). Tropical Indian Ocean influence on northwest Pacific tropical cyclones in summer following strong El Niño. *J. Climate* 24, 315–322. doi: 10.1175/2010JCLI3890.1

Gao, J., Hou, L., Liu, Y., and Shi, H. (2024). Influences of bragg reflection on harbor resonance triggered by irregular wave groups. *Ocean Eng.* 305, 117941. doi: 10.1016/j.oceaneng.2024.117941

Gao, J., Ji, C., Gaidai, O., Liu, Y., and Ma, X. (2017). Numerical investigation of transient harbor oscillations induced by N-waves. *Coast. Eng.* 125, 119–131. doi: 10.1016/j.coastaleng.2017.03.004

Gao, J., Ma, X., Dong, G., Chen, H., Liu, Q., and Zang, J. (2021). Investigation on the effects of Bragg reflection on harbor oscillations. *Coast. Eng.* 170, 103977. doi: 10.1016/j.coastaleng.2021.103977

Gao, J., Shi, H., Zang, J., and Liu, Y. (2023). Mechanism analysis on the mitigation of harbor resonance by periodic undulating topography. *Ocean Eng.* 281, 114923. doi: 10.1016/j.oceaneng.2023.114923

Geng, X., Jiang, W., Zhang, M., Liu, W., and Liu, X. (2024). Characteristics of phytoplankton assemblages and their relationship with environmental factors in the Qiongzhou Strait, China. *Mar. pollut. Bull.* 205, 116560. doi: 10.1016/j.marpolbul.2024.116560

Grebmeier, J. M., Cooper, L. W., Feder, H. M., and Sirenko, B. I. (2006). Ecosystem dynamics of the Pacific-influenced northern Bering and Chukchi Seas in the Amerasian Arctic. *Prog. Oceanography* 71, 331–361. doi: 10.1016/j.pocean.2006.10.001

Hernández-Molina, F. J., Stow, D. A., Alvarez-Zarikian, C. A., Acton, G., Bahr, A., Balestra, B., et al. (2014). Onset of Mediterranean outflow into the North Atlantic. *Science* 344, 1244–1250. doi: 10.1126/science.1251306

Hu, J. Y., Kawamura, H., and Tang, D. L. (2003). Tidal front around the Hainan Island, northwest of the South China Sea. *J. Geophysical Res.: Oceans* 108. doi: 10.1029/2003JC001883

Jerlov, N. G. (1968). *Optical oceanography* Vol. 5 (Amsterdam, Netherlands: Elsevier).

Jing, Z., Qi, Y., and Du, Y. (2011). Upwelling in the continental shelf of northern South China Sea associated with 1997–1998 El Niño. *J. Geophysical Res.: Oceans* 116. doi: 10.1029/2010JC006598

Lao, Q., Zhang, S., Li, Z., Chen, F., Zhou, X., Jin, G., et al. (2022). Quantification of the seasonal intrusion of water masses and their impact on nutrients in the Beibu Gulf using dual water isotopes. *J. Geophysical Res.: Oceans* 127, e2021JC018065. doi: 10.1029/2021JC018065

Li, J., Bai, P., Zhai, F., Gu, Y., Li, P., Liu, C., et al. (2024). Decadal variation in winter-spring thermal front to the Zhejiang-Fujian coast and its mechanism. *J. Geophysical Res.: Oceans* 129, e2023JC020671. doi: 10.1029/2023JC020671

Liang, X., and Wu, L. (2013). Effects of solar penetration on the annual cycle of sea surface temperature in the North Pacific. *J. Geophysical Res.: Oceans* 118, 2793–2801. doi: 10.1002/jgrc.v118.6

Lin, P., Cheng, P., Gan, J., and Hu, J. (2016). Dynamics of wind-driven upwelling off the northeastern coast of Hainan Island. *J. Geophysical Res.: Oceans* 121, 1160–1173. doi: 10.1002/2015JC011000

Morel, A. (1988). Optical modeling of the upper ocean in relation to its biogenous matter content (case I waters). *J. Geophysical Res.: Oceans* 93, 10749–10768. doi: 10.1029/JC093iC09p10749

Ni, Y., Endler, R., Xia, Z., Endler, M., Harff, J., Gan, H., et al. (2014). The "butterfly delta" system of Qiongzhou Strait: Morphology, seismic stratigraphy and sedimentation. *Mar. Geol.* 355, 361–368. doi: 10.1016/j.margeo.2014.07.001

Paulson, C. A., and Simpson, J. J. (1977). Irradiance measurements in the upper ocean. *J. Phys. Oceanography* 7, 952–956. doi: 10.1175/1520-0485(1977)007<0952:IMITUO>2.0.CO;2

Qu, T. (2003). Mixed layer heat balance in the western North Pacific. *J. Geophysical Res.: Oceans* 108. doi: 10.1029/2002JC001536

Shi, M., Chen, C., Xu, Q., Lin, H., Liu, G., Wang, H., et al. (2002). The role of Qiongzhou Strait in the seasonal variation of the South China Sea circulation. *J. Phys. Oceanography* 32, 103–121. doi: 10.1175/1520-0485(2002)032<0103:TROQSI>2.0.CO;2

Swingedouw, D., Colin, C., Eynaud, F., Ayache, M., and Zaragosi, S. (2019). Impact of freshwater release in the Mediterranean Sea on the North Atlantic climate. *Climate Dynamics* 53, 3893–3915. doi: 10.1007/s00382-019-04758-5

Van Maren, D. S., and Gerritsen, H. (2012). Residual flow and tidal asymmetry in the Singapore Strait, with implications for resuspension and residual transport of sediment. *J. Geophysical Res.: Oceans* 117. doi: 10.1029/2011JC007615

Wang, S., Jing, Z., Wu, L., Sun, S., Peng, Q., Wang, H., et al. (2023). Southern hemisphere eastern boundary upwelling systems emerging as future marine heatwave hotspots under greenhouse warming. *Nat. Commun.* 14, 28. doi: 10.1038/s41467-022-35666-8

Wang, Q., Wang, X., Xie, L., Shang, Q., and Lü, Y. (2014). Observed water current and transport through Qiongzhou Strait during August 2010. *Chin. J. Oceanol. Limnol.* 32, 703–708. doi: 10.1007/s00343-014-3159-6

Woodgate, R. A., Aagaard, K., and Weingartner, T. J. (2005). Monthly temperature, salinity, and transport variability of the Bering Strait through flow. *Geophysical Res. Lett.* 32. doi: 10.1029/2004GL021880

Woodgate, R. A., Weingartner, T. J., and Lindsay, R. (2012). Observed increases in Bering Strait oceanic fluxes from the Pacific to the Arctic from 2001 to 2011 and their impacts on the Arctic Ocean water column. *Geophysical Res. Lett.* 39. doi: 10.1029/2012GL054092

Wu, D., Wang, Y., Lin, X., and Yang, J. (2008). On the mechanism of the cyclonic circulation in the Gulf of Tonkin in the summer. *J. Geophys. Res.: Oceans* 11 (C9). doi: 10.1029/2007JC004208

Xie, S. P., Du, Y., Huang, G., Zheng, X. T., Tokinaga, H., Hu, K., et al. (2010). Decadal shift in El Niño influences on Indo–western Pacific and East Asian climate in the 1970s. *J. Climate* 23, 3352–3368. doi: 10.1175/2010JCLI3429.1

Xie, S. P., Hu, K., Hafner, J., Tokinaga, H., Du, Y., Huang, G., et al. (2009). Indian Ocean capacitor effect on Indo–western Pacific climate during the summer following El Niño. *J. Climate* 22, 730–747. doi: 10.1175/2008JCLI2544.1

Yang, J., Jiang, S., Wu, J., Xie, L., Zhang, S., and Bai, P. (2020). Effects of wave-current interaction on the waves, cold-water mass and transport of diluted water in the Beibu Gulf. *Acta Oceanologica Sinica*. 39, 25–40. doi: 10.1007/s13131-019-1529-9

Yan, C., Chen, B., Yang, S., and Yan, J. (2008). The transportation volume of water through the Qiongzhou Strait in winter season. *Trans. Oceanol. Limnol.* 1, 1–9. doi: 10.13984/j.cnki.cn37-1141.2008.01.010

Yang, S., Bao, X., Chen, C., and Chen, F. (2003). Analysis on characteristics and mechanism of current system in west coast of Guangdong Province in the summer. *Acta Oceanol. Sin.* 25, 1–8.

Zavala-Garay, J., Rogowski, P., Wilkin, J., Terrill, E., Shearman, R. K., and Tran, L. H. (2022). An integral view of the Gulf of Tonkin seasonal dynamics. *J. Geophysical Res.: Oceans* 127, e2021JC018125. doi: 10.1029/2021JC018125

Zhang, Y., Du, Y., Feng, M., and Hobday, A. J. (2023). Vertical structures of marine heatwaves. *Nat. Commun.* 14, 6483. doi: 10.1038/s41467-023-42219-0

Zheng, Q., Wang, H., Li, S., Cao, Z., and Bao, M. (2024). Dynamics of currents in the Qiongzhou strait during spring and summer based on a numerical simulation. *Front. Mar. Sci.* 11, 1367145. doi: 10.3389/fmars.2024.1367145

Zhu, X. H., Ma, Y. L., Guo, X., Fan, X., Long, Y., Yuan, Y., et al. (2014). Tidal and residual currents in the Q iongzhou S trait estimated from shipboard ADCP data using a modified tidal harmonic analysis method. *J. Geophysical Res.: Oceans* 119, 8039–8060. doi: 10.1002/2014JC009855

Zhu, X. H., Zhu, Z. N., Guo, X., Ma, Y. L., Fan, X., Dong, M., et al. (2015). Measurement of tidal and residual currents and volume transport through the Qiongzhou Strait using coastal acoustic tomography. *Continental Shelf Res.* 108, 65–75. doi: 10.1016/j.csr.2015.08.016